The Application of Theoretical Diffusion Models in the Presence of a Catalytic Reaction

J. S. STERRETT and L. F. BROWN

University of Colorado, Boulder, Colorado

The fundamental problem in this work was to determine if methods of predicting mass transport rates in porous catalysts, developed from theory in the absence of chemical reaction, are valid in the presence of reaction. By using the ortho-para shift of hydrogen over a ferric oxide gel catalyst as the reacting system, the effective diffusivity within the catalyst was determined from kinetic data on five different particle sizes of the catalyst. This effective diffusivity was then compared with that predicted by three different procedures recently published. These procedures predicted diffusivities approximately 40% below the experimentally obtained diffusivity. Although the differences between the experimental and predicted effective diffusivities can be regarded as within the limitations of the accuracy of the predictions, the observed differences may also be caused by some form of surface transport.

In 1939, Thiele in the United States (*17*) and Zeldowitsch in the U.S.S.R. (*24*) simultaneously published pioneering contributions concerning the effect on a catalytically promoted chemical reaction of diffusion within the pores of a solid catalyst. Since these contributions, calculation of effective diffusivities from pore structure parameters has been a common practice. The purpose of this study was to investigate whether the present means of predicting diffusion rates inside microporous substances from the pore structure are applicable for diffusion in the presence of a catalytic reaction. Certain models have been shown to predict diffusion rates apparently within ± 50% in the absence of reaction where the models were compared with direct diffusion measurements (*10, 21*). However, Satterfield and Sherwood in a comprehensive review of diffusion in catalysis through early 1963 (*15*) stated, "There is still considerable uncertainty as to the conditions under which flow or diffusion measurements through porous catalysts can be used to calculate effective diffusion coefficients for the problem of diffusion and reaction within the catalyst structure."

In this study, orthohydrogen was reacted to parahydrogen on microporous ferric oxide gel, which has a reasonably narrow pore size distribution. The reaction was conducted under conditions where diffusion affected the overall reaction rate so that the overall reaction rate was dependent upon the nature of the micropore structure. The effective diffusivity was calculated from the theory on diffusion and reaction within a catalyst. This diffusivity was compared with predicted effective diffusivity values from the present diffusion models which are based solely on catalyst pore structure.

This investigation required pore structure measurements and activity measurements for different particle sizes. The pore structure of most porous catalysts is characterized by a myriad of minute intersecting pores which provide a large surface area for reaction. If the particle size of the catalyst is sufficiently large, diffusion of reactants and products through such a labyrinth of intersecting pores may reduce or even control the overall reaction rate.

Reaction rates have been used by other investigators to determine effective diffusion rates within porous catalysts. Weisz and Swegler (*22*) calculated effective diffusivities using the dehydrogenation of cyclohexane; Weisz and Prater (*20*) used the cracking of cumene; and Johnson, Kreger, and Erickson (*9*) determined the effective diffusivities from the cracking of gas oil. All these studies were carried out over microporous catalysts, but the first two did not present sufficient data on the catalysts to calculate theoretical diffusion rates from the current models. The work of Johnson, et al. gave a very complete description of the catalysts, but the reaction studied is so complex that the precision of any results would be open to some doubt. An investigation somewhat similar to the present one was carried out by Rao, Wakao, and Smith (*14*) using the ortho-parahydrogen shift on bimodal catalysts with large macropore contributions. In 1962, Wakao and Smith postulated a model for diffusion in bidisperse pore systems (*19*) and extended this model in 1964 to simultaneous diffusion and reaction in bidisperse pore systems (*18*). The experimental work of Rao, Wakao, and Smith supported this latter model, but they admonished that the theory may not be applicable for a microporous catalyst.

THEORY

Diffusion inside the tortuous void passages of a porous catalyst is complex and difficult to visualize. In situations where Knudsen flow is assumed to predominate, the mathematical approach to this problem has been to apply Fick's law and a mass balance to a differential volume of catalyst. For an equimolar isothermal first-order reaction, this results in a linear second-order differential equation for simplified particle geometries. Thiele (*17*) derived the equations for both spherical particles and thin slab particles with sealed edges. This analysis defined a dimensionless modulus, called the *Thiele Modulus*, which characterizes the system.

The catalyst particles used in this study were irregularly shaped granules, and it was necessary to choose an approximate shape to characterize these granules for mathematical treatment. The diffusion models for a sphere and

J. S. Sterrett is with Gulf Research and Development Company, Pittsburgh, Pennsylvania.

a thin slab represent idealized models of extreme particle geometry. The sphere model describes three-dimensional diffusion through catalyst particles whereas the thin slab model with sealed edges is based on only one-dimensional diffusion. The latter model may be acceptable for a strongly diffusion-limited system where the reaction occurs near the exterior surface. This model is inadequate, however, for an intermediate region between the strongly diffusion-limited region and the surface reaction-limited region (2). Since the experimental reaction rates in the present study were measured in this intermediate region, the sphere model was used for the mathematical analysis.

The model for simultaneous diffusion and reaction in a sphere is presented in the following development. This development assumes an isothermal first-order reversible reaction with either equimolar counter-diffusion or Knudsen diffusion.

A spherical catalyst particle of radius, R_p, is assumed. A steady state material balance over a spherical shell, r_p, gives:

$$-D_e(4\pi r_p^2)\frac{dC_A}{dr_p} - (4\pi r_p^2)\delta r_p\, Sk_s\,(C_A - C_{Ae}) = -D_e\left[4\pi r_p^2 + \frac{d(4\pi r_p^2)}{dr_p}\delta r_p\right]\frac{d}{dr_p}\left(C_A + \frac{dC_A}{dr_p}\delta r_p\right) \quad (1)$$

Simplification of the above expression yields the following second-order linear differential equation:

$$\frac{d^2C_A}{dr_p^2} + \frac{2}{r_p}\frac{dC_A}{dr_p} - \frac{k_sS}{D_e}(C_A - C_{Ae}) = 0 \quad (2)$$

If we define

$$h_{sp} = \text{Thiele Modulus} = \frac{R_p}{3}\sqrt{\frac{k_sS}{D_e}}$$

The solution of the above equation with the boundary conditions $C_A = C_{Ao}$ at $r_p = R_p$ and $dC_A/dr_p = 0$ at $r_p = 0$, is

$$\frac{C_A - C_{Ae}}{C_{Ao} - C_{Ae}} = \frac{R_p}{r_p}\frac{\sinh(3r_ph_{sp}/R_p)}{\sinh(3h_{sp})} \quad (3)$$

The reaction rate for one sphere equals the rate of diffusion across the exterior surface, thus

$$(\text{reaction rate/sphere}) = 4\pi R_p^2 D_e \left.\frac{dC_A}{dr_p}\right|_{r_p=R_p} \quad (4)$$

Differentiation of Equation (3) with respect to r_p, evaluated at $r_p = R_p$, yields

$$\left.\frac{dC_A}{dr_p}\right|_{r_p=R_p} = \left[\frac{3h_{sp}}{R_p\tanh(3h_{sp})} - \frac{1}{R_p}\right](C_{Ao} - C_{Ae}) \quad (5)$$

Therefore

$$(\text{reaction rate/sphere}) = 4\pi R_pD_e\left[\frac{3h_{sp}}{\tanh(3h_{sp})} - 1\right](C_{Ao} - C_{Ae}) \quad (6)$$

Since the catalyst volume occupied by one sphere is equal to $(4\pi R_p^3/3)$, the reaction rate per catalyst volume is

$$(\text{reaction rate/catalyst volume}) = \frac{3D_e}{R_p^2}(C_{Ao} - C_{Ae})\left[\frac{3h_{sp}}{\tanh(3h_{sp})} - 1\right] \quad (7)$$

Substitution of the reaction rate into the plug flow reactor design equation:

$$FdC_{Ao} = -\bar{R}dV_C \quad (8)$$

gives

$$FdC_{Ao} = -\frac{3D_e}{R_p^2}(C_{Ao} - C_{Ae})\left[\frac{3h_{sp}}{\tanh(3h_{sp})} - 1\right]dV_C \quad (9)$$

Integration of this equation and transposing the result gives D_e implicitly with h_{sp} a function of D_e:

$$D_e = \frac{\frac{R_p^2}{3}\frac{F}{V_C}\ln\frac{(C_{Ao} - C_{Ae})_{\text{inlet}}}{(C_{Ao} - C_{Ae})_{\text{outlet}}}}{\frac{3h_{sp}}{\tanh 3h_{sp}} - 1} \quad (10)$$

This fundamental equation describes simultaneous diffusion and reaction. When D_e is known or can be predicted, the Thiele Modulus can be determined from basic kinetic data (conversion and space velocity) and the average particle size of the catalyst.

If kinetic data are available for two or more particle sizes, D_e can theoretically be extracted from Equation (10). Let the subscript, X, denote one particle size; let the subscript, Y, denote another particle size. Then, the proportion, $(h_{spX}/h_{spY}) = R_{pX}/R_{pY}$, is valid. Assuming D_e is constant, the Thiele Moduli for two particle sizes can be evaluated by a trial and error process from the known proportion of the Thiele Moduli and from the ratio resulting from the use of Equation (10), thus

$$\frac{\frac{3h_{spX}}{\tanh 3h_{spX} - 1}}{\frac{3h_{spY}}{\tanh 3h_{spY} - 1}} = \frac{\left[\frac{R_p^2}{3}\frac{F}{V_C}\ln\frac{(C_{Ao} - C_{Ae})_{\text{inlet}}}{(C_{Ao} - C_{Ae})_{\text{outlet}}}\right]_X}{\left[\frac{R_p^2}{3}\frac{F}{V_C}\ln\frac{(C_{Ao} - C_{Ae})_{\text{inlet}}}{(C_{Ao} - C_{Ae})_{\text{outlet}}}\right]_Y}$$

After the Thiele Modulus is obtained, D_e can be calculated directly from Equation (10).

The significance of intraparticle diffusion (diffusion within the catalyst particles) on a chemical reaction is measured by the effectiveness factor, which is the ratio of the actual reaction rate to the reaction rate neglecting the diffusional resistance. The effectiveness factor for a spherical catalyst pellet (24) is

$$E = \frac{1}{h_{sp}}\left[\frac{1}{\tanh 3h_{sp}} - \frac{1}{3h_{sp}}\right] \quad (12)$$

The equations analogous to Equations (10) and (11) for a slab model of a catalyst pellet have been derived and presented by one of the authors (16). These would be used in circumstances of strong intraparticle diffusion limitation because of their mathematical simplicity.

DIFFUSION MODELS

In 1962, Weisz and Schwartz (21) developed a pore model for predicting effective diffusivities in gel-derived catalysts in the absence of a chemical reaction. From the Weisz and Schwartz data on 46 unimodal catalysts the model predicted effective diffusivities with a maximum deviation from the measured diffusivities of +89.7%, −17.2%, and an average percent deviation from the measured diffusivities of 27.6%. Haynes (6) evaluated an empirical correction factor ($f = 0.758$) from a linear regression analysis of the Weisz and Schwartz data. The use of this correction factor on the data yielded a maximum deviation from the measured diffusivities of +43.9%, −37.4%, and an average percent deviation from the measured diffusivities of 17.4%.

By using a concept of overlapping spherical cells, Weisz and Schwartz developed an expression for the diffusivity under conditions of Knudsen flow:

$$D_{pre} = (2/3)(1/\sqrt{3})\,\alpha^2\,\bar{v}\,\bar{r} \qquad (13)$$

Since spherical shaped pores were assumed, the mean pore radius was further defined by $\bar{r} = 3p_v/S_t$. Also, $\alpha = d_p p_v$ where d_p is the particle density. The mean molecular velocity can be calculated from the kinetic theory of gases (5). For hydrogen at 75.7°K., $\bar{v}$ is 8.916×10^4 cm./sec.

The predicted effective diffusivity of hydrogen at 75.7°K. for the Weisz and Schwartz model may then be expressed by

$$D_{pre} = (1.0396 \times 10^5)\, d_p^2 p_v^3 / S_t \qquad (14)$$

This model requires only the particle density, pore volume, and surface area.

The empirical correction factor evaluated by Haynes can be partially justified by a theoretical modification of the Weisz and Schwartz model. The Weisz and Schwartz model can be modified by $1/\sqrt{3}$ to change the tortuosity factor from $\sqrt{3}$, which was used, to three, which is the correct value for randomly oriented cylindrical pores with no dead ends in an isotropic pore system.

Johnson and Stewart (10) predicted effective diffusivities by integration of predicted diffusion rates for the entire distribution of pore sizes. This model was developed in 1964 primarily to predict diffusion rates for bimodal or wide pore size distributions, for example, for pelleted or extruded catalysts. Johnson and Stewart supported the model with experimentally measured diffusivities in the absence of a chemical reaction. For eleven bimodal catalysts, diffusivities were predicted with a maximum deviation from the measured diffusivities of +127.4%, −12.9%, and an average percent deviation from the measured diffusivities of 48.5%. Also, effective diffusivities were predicted for eight unimodal catalysts with a maximum deviation from the measured diffusivities of +11.8%, −27.7%, and an average percent deviation from the measured diffusivities of 13.5%.

The Johnson and Stewart model simplifies greatly for equimolar countercurrent diffusion, which is exhibited in the binary diffusion of orthohydrogen and parahydrogen. These authors derived an expression for $N_{Az}L$ based on the pore orientation and the pore size distribution:

$$N_{Az}L = -K\int_o^\infty \int_{x_{Ao}}^{x_{AL}} B^{-1}\,dx_A f(r)\,dr$$

$$\text{with } B^{-1} = \left\{ \frac{1 + x_A[(M_A/M_B)^{1/2} - 1]}{CD_{AB}} + \frac{1}{CD_K} \right\}^{-1} \qquad (15)$$

With equimolal countercurrent diffusion, B^{-1} reduces to

$$B^{-1} = C\left\{ \frac{1}{D_{AB}} + \frac{1}{D_K} \right\}^{-1} \qquad (16)$$

Substitution for B^{-1} and evaluation of the inner integral gives

$$N_{Az}L = CK(x_{Ao} - x_{AL}) \int_o^\infty \frac{f(r)\,dr}{\frac{1}{D_{AB}} + \frac{1}{D_K}} \qquad (17)$$

The Knudsen diffusivity is evaluated from the relationship for transport within long cylindrical tubes (24):

$$D_K = (2r/3)(\bar{v}) \qquad (18)$$

The molecular self-diffusivity of hydrogen at 75.7°K. and 20 lb./sq. in. is 0.057 sq. cm./sec. from Equation (4) for estimating D_{AB} at low pressures.

By definition, the effective diffusivity is

$$D_{pre} = \frac{N_{Az}L}{(C_{Ao} - C_{AL})} \qquad (19)$$

Substitution of Equation (17) into Equation (19) provides the following expression for effective diffusivity:

$$D_{pre} = K\int_o^\infty \frac{f(r)\,dr}{\frac{1}{D_{AB}} + \frac{1}{D_K}} \qquad (20)$$

The void fraction in pores with radii between r and $r + dr$ can be approximated graphically by the product of the particle density (d_p) and the incremental pore volume (Δp_v) between r and $r + \Delta r$. Therefore

$$D_{pre} \approx K d_p \sum_{r=0}^{r=\infty} \frac{\Delta p_v}{\frac{1}{D_{AB}} + \frac{1}{D_K}} \qquad (21)$$

This form of the Johnson and Stewart model was used in the present work to determine the predicted diffusivity.

The pore orientation parameter (K) was assumed to be 1/3, which is the correct parameter for randomly oriented cylindrical pores with no dead ends in an isotropic pore system. The experimental support of the Johnson and Stewart model that was stated earlier was based on this pore orientation parameter.

One other model for diffusion within porous catalysts based solely on catalyst pore structure was proposed by Wakao and Smith (19) specifically for transport within bimodal catalysts. There have been very few applications of this model to purely microporous materials. Henry, et al. (7) showed that the predicted and measured diffusivities through a sample of Vycor agreed very well over a pressure range of 0.6 to 600 mm. mercury abs., with a maximum deviation of + 26% at the highest pressure. However, Rao and Smith (13), also using a sample of Vycor, predicted a value of the effective diffusivity 70% higher than the experimental value.

Wakao and Smith's model is a summation of three parallel mechanisms. These are diffusion in the micropore region, diffusion in the macropore region, and diffusion in the micro-macropore region. The model is greatly simplified for equimolar counterdiffusion in a purely microporous catalyst. The rate of diffusion in a cylindrical micropore at constant pressure in a binary system of gases A and B is

$$N_{Az} = -\frac{1}{\frac{1}{D_{AB}} + \frac{1}{D_K}} \frac{dC_A}{dz} \qquad (22)$$

The porosity squared is introduced for the rate of diffusion in a porous particle. The resulting predicted diffusivity is

$$D_{pre} = \frac{\alpha^2}{\frac{1}{D_{AB}} + \frac{1}{D_K}} \qquad (23)$$

The average radius for the Knudsen diffusivity is evaluated from the relationship (19):

$$\bar{r} = \frac{\int_o^{V_p} r\,dV_p}{V_p} \qquad (24)$$

DESCRIPTION OF APPARATUS

Two types of data were obtained in this investigation: kinetic data for the reaction and data on the catalyst structure for the purpose of predicting the diffusional processes of the catalyst.

Apparatus for Determination of Reaction Rates

The apparatus used to obtain the kinetic data consisted of feed preparation, reactor, and analysis sections. A schematic diagram of the apparatus is shown in Figure 1.

The hydrogen feed, which was an ultra pure grade hydrogen contained less than 10 ppm. impurities. A silica gel bed for the removal of impurities and a hydrogen normalizer to insure compositional uniformity were installed in the feed stream. The silica gel bed was immersed in a bath of liquid nitrogen. Following passage through the silica gel, the hydrogen was then passed through a normalizer. The normalizer, which converted hydrogen to its normal composition of 25% parahydrogen and 75% orthohydrogen, contained a nickel catalyst at 500°C. The normal hydrogen was the feed for the reactor and the reference gas for the analyzer.

The flow reactor was a ¼ in. O.D. copper tube, 2.5 in. in length. The inlet and outlet of the tubular reactor were packed with pyrex wool to contain the ferric oxide gel. When activating the catalyst, the reactor was immersed in a constant temperature oil bath that was regulated by a Fenwal Thermoswitch; when carrying out the reaction, the reactor was immersed in a dewar filled with liquid nitrogen. The hydrogen feed was cooled to the reaction temperature by passing through a ⅛ in. copper feed line coiled around the reactor. Pressure gauges were also placed on the reactor inlet and outlet streams.

A thermal conductivity analyzer was used to determine the orthopara conversion. The conversion was recorded on a Speedomax H strip chart recorder. The hydrogen flow rate was measured with a wet test meter.

Apparatus for Determination of Pore Structure

Two pieces of apparatus were used in determination of the catalyst pore structure. One was an Aminco Porosimeter, 15,000 lb./sq. in. model. The other apparatus was a Numinco-Orr Surface Area-Pore Volume Analyzer, model MIC 101. Descriptions and specifications of these pieces of apparatus are obtainable in the literature (*1, 11*).

PROCEDURE

The experimental procedure for the determination of the effects of diffusion on reaction rates entailed activation of the catalyst and measurement of the catalyst activity for a variety of catalyst particle sizes. Also, the prediction models for diffusion required measurements of the pore structure of the catalyst.

Catalyst

The catalyst used in this study was a hydrous ferric oxide catalyst developed by Weitzel and Loebenstein (*23*). All the catalyst that was used was from the same batch. The catalyst particles were crushed into the following Tyler sieve sizes: 30-40 mesh, 40-50 mesh, 50-60 mesh, 60-80 mesh, and 80-100 mesh.

The activation conditions were chosen from a previous extensive activation study carried out by Barrick, et al. (*3*) to promote the orthopara shift of hydrogen on the hydrous ferric oxide catalyst. This study revealed that the high activities obtained when the catalyst was activated at temperatures greater than 250°C. for short periods of time (approximately 5 min.) were not always reproducible. Since reproducible activities were essential for this work, a milder activation procedure was selected which produced an acceptably reproducible intermediate activity.

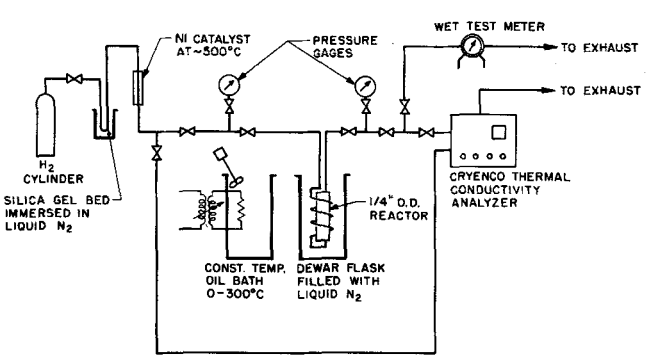

Fig. 1. Activity testing apparatus.

For the catalyst activation, the oil bath was set at a constant temperature of 120°C. A flow of hydrogen from the silica gel trap and normalizer was passed over the catalyst under a pressure of 10 lb./sq. in. gauge at a rate of 150 cc. (STP)/min./volume of catalyst. The actual activation commenced when the reactor was immersed in the 120°C. oil bath. An activation time of 4 hr. was used after which the reactor was removed from the oil bath to terminate the activation.

Activity Measurements

For each run, the hydrogen flow rate through the reactor was increased incrementally. The runs were carried out at 32 lb./sq. in. abs. and 76°K. Measurements of flow rate and outlet composition were taken at each point. One data point specifically was taken to determine the activity, which was arbitrarily defined as the flow rate corresponding to an exit composition of 42% parahydrogen. This procedure provided all the essential data for interpretation of the system.

Each catalyst was activated twice, and each average particle size was run in duplicate. After the final activity measurements were determined, each activated catalyst was weighed, then placed in a desiccator. Complete details of the procedure are presented by one of the authors (*16*).

Pore Structure Determination

The procedures for using the mercury porosimeter and the nitrogen adsorption apparatus are outlined extensively in the respective instruction manuals (*1, 11*). The only specific information not contained in the instruction manual is the degassing conditions for the nitrogen adsorption. The samples were degassed under a vacuum at 120°C. for 4 hr. Treatment at different temperatures is shown to have a marked effect on catalyst activity (3), and thus presumably some effect on the catalyst structure. Therefore, degassing conditions were selected as close as possible to the activation conditions.

RESULTS

The activity measurements for all the runs are shown in Table 1. Each catalyst was activated twice, and duplicate runs were made on each particle size. The deviations

TABLE 1. ACTIVITY MEASUREMENTS

Activation conditions:	Time	4 hr.
	Temp.	120°C.
	Pressure	10 lb./sq.in.gauge
	Flowing hydrogen	150 cc. (STP)/min.—vol. cat.

Activity definition:

The activity of the catalyst was arbitrarily defined as the volume of hydrogen (STP)/min. per unit catalyst volume required to convert 75% orthohydrogen to 58% orthohydrogen at 75.7°K.

Run	Mesh size	Avg. diam. in.	Initial activity min.$^{-1}$	Second activity min.$^{-1}$	Avg. second activity min.$^{-1}$
30-01	30-40	0.0180	5,640	6,100	6,165
30-02			6,330	6,230	
40-01	40-50	0.0130	6,460	6,850	6,800
40-02			6,450	6,750	
50-01	50-60	0.0106	6,700	7,100	7,080
50-03			6,820	7,060	
60-01	60-80	0.0084	7,410	7,300	7,270
60-03			7,240	7,240	
80-01	80-100	0.0064	7,300	7,580	7,615
80-02			7,580	7,650	

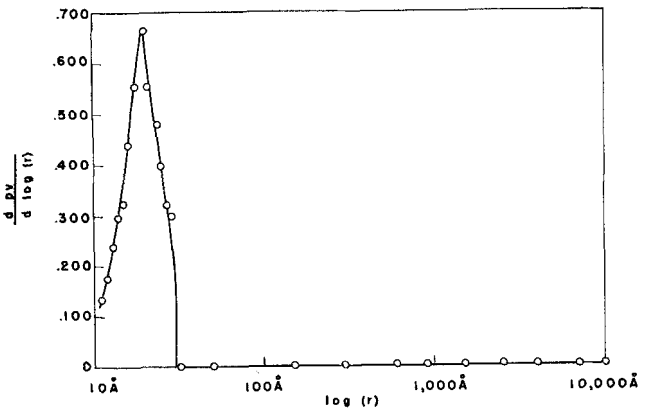

Fig. 2. Pore size distribution catalyst 30-02.

from the averages of the activity measurements for identical particle sizes were as high as 5.7% for the first activation whereas a maximum deviation of only ± 1% was observed for the second activation. A second activation therefore greatly improved the reproducibility.

The effective diffusivity was extracted from the models by treating the Thiele Modulus for the 80-100 mesh catalyst as an adjustable parameter. A value for the Thiele Modulus for this catalyst was first assumed, and then the Thiele Moduli for the other particle sizes were calculated from the ratio of the respective radii. The effective diffusivity was evaluated for each particle size from Equation (10). The assumed value for the Thiele Modulus for the 80-100 mesh catalyst was then varied until the minimum statistical variance of the effective diffusivities for the five particle sizes was obtained. These effective diffusivities are listed in Table 2. The average deviation from the mean effective diffusivity for the sphere model was 0.701%, and maximum deviations observed were +0.935%, −1.14%. Effectiveness factors were also evaluated from the Thiele Moduli.

For the purpose of predicting diffusivities from theoretical models, the pore structure parameters shown in Table 3 were used. Branauer-Emmett-Teller (BET) surface areas and pore-size distributions for pores below 100 Å. were obtained from the nitrogen adsorption isotherms. The mercury porosimeter data indicated no significant amount of pores present with radii above 70 Å. The BET surface areas, particle densities, pore volumes, and cumulative pore volumes and cumulative surface areas from the pore-size distribution are presented in Table 3. The pore-size distribution, presented in Figure 2, indicates the activated hydrous ferric oxide catalyst is microporous with a unimodal pore-size distribution. The complete mercury porosimeter and nitrogen adsorption data are presented by one of the authors (*16*).

Table 2. Sphere Model Diffusivities

Particle size mesh	Thiele modulus	Effectiveness factor	Effective diffusivity sq.cm./sec. × 10^4	Max. activity min.$^{-1}$
30-40	0.725	0.7845	19.36	7,850
40-50	0.529	0.8689	19.27	7,840
50-60	0.431	0.9071	19.23	7,810
60-80	0.339	0.9387	19.05	7,750
80-100	0.257	0.9630	19.45	7,900

Avg. diffusivity	19.27×10^{-4} sq.cm./sec.
Diffusivity variance	0.01820×10^{-8} (sq.cm/sec.)^2
Avg. max. activity	7830 min.$^{-1}$
Avg. deviation of diffusivity	0.701%
Max. deviations of diffusivity	+0.935%, −1.14%

Table 3. Pore Structure Parameters

		Avg. values
BET surface area (S_t), sq.m./g.		
Catalyst 80-02	225	
Catalyst 30-02	220	222
Particle density from the mercury porosimeter (d_p), g./cc.		
Catalyst 40-02	2.09	
Catalyst 50-03	2.03	2.06
Pore volume from the nitrogen adsorption isotherm (p_v), cc./g.		
Catalyst 80-02	0.201	
Catalyst 30-02	0.196	0.198
Calculated from pore-size distributions:		
Cumulative pore volume (p_v), cc./g., down to a radius of:	10 Å	5.2 Å
Catalyst 80-02	0.189	0.206
Catalyst 30-02	0.177	0.199
Cumulative surface area (S_t), sq.m/g., down to a radius of:	10 Å	5.2 Å
Catalyst 80-02	203	249
Catalyst 30-02	185	243

For the data obtained in this investigation to be significant, the different catalyst particles would have to exhibit the same pore structure. This is affirmed in Figure 3 which depicts the nitrogen adsorption isotherms of two extreme particle sizes, 30-40 mesh and 80-100 mesh. The resulting isotherms are nearly identical.

The diffusivity values from the diffusion models of Weisz and Schwartz, Johnson and Stewart, and Wakao and Smith are listed in Table 4 along with the modification mentioned in the theory section. Further evidence of the similarity of pore structures can be seen from the close values of the predicted effective diffusivities for the different particles. The predicted diffusivities from the various theoretical models were significantly below the diffusivities calculated from the experimental data.

The reliability of the pore-size distribution curves becomes extremely questionable at low radii (*12*), so two

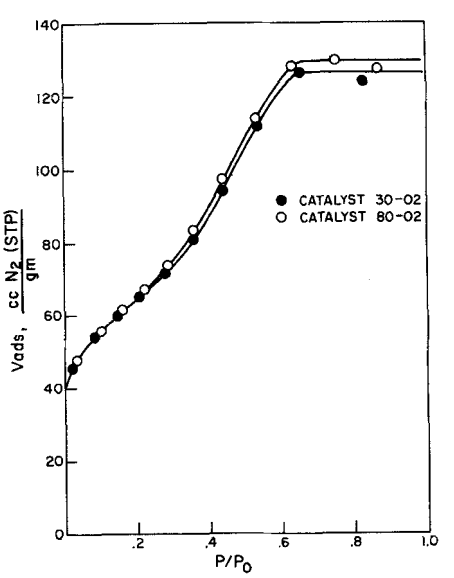

Fig. 3. Nitrogen adsorption isotherm (75.7°K.).

different radii were used as the cutoff point. The use of a wider distribution made little difference in the diffusivities predicted by the Johnson and Stewart model, but did make a noticeable difference in the predictions of the Wakao and Smith model. In no case, however, did the predicted diffusivities approach the experimental diffusivity.

TABLE 4. PREDICTED EFFECTIVE DIFFUSIVITIES

Model	Weisz & Schwartz	W. & S. with tortuosity correction of 0.758	Johnson & Stewart	Wakao & Smith
	Diffusivity $\times 10^4$, sq.cm./sec.			
Catalyst 30-02				
To a radius of 10 Å.	15.1	11.4	10.8	11.4
To a radius of 5.2 Å.			11.5	14.0
Catalyst 80-02				
To a radius of 10 Å.	15.9	12.0	11.4	12.7
To a radius of 5.2 Å.			11.9	15.1

Experimental effective diffusivity: 19.3×10^{-4} sq.cm./sec.

DISCUSSION OF RESULTS

Some criterion of reliability of the experimental effective diffusivities in this study should be offered. Since two different particle sizes are required for the effective diffusivity to be calculated, the use of five particle sizes offered a fourfold redundancy in calculating the effective diffusivity. The calculated diffusivities presented a maximum deviation less than ± 1.2% from the mean diffusivity, and an average deviation of 0.70%. The small deviations of the calculated diffusivities over the large range of particle sizes is regarded as evidence of the reproducibility and internal consistency of the experimental results.

All three theoretical models predicted effective diffusivities significantly lower than the experimental diffusivities. The Weisz and Schwartz model modified by the empirical correction factor ($f = 0.758$) recommended by Haynes predicted an effective diffusivity approximately 40% below the experimental value. Since this modification of the Weisz and Schwartz model predicted effective diffusivities of 46 microporous catalysts within 38% below the measured diffusivity, the 40% deviation observed in this study is only slightly greater than the maximum error observed previously in absence of reaction.

The effective diffusivity predicted from the Johnson and Stewart diffusion model was also approximately 40% below the experimental diffusivity. Experimental data by Johnson and Stewart supported their model within 28% below diffusivities measured on microporous catalysts in the absence of reaction. However, this maximum deviation was only for eight samples as compared with the 46 samples for the Weisz and Schwartz model.

The Wakao and Smith diffusion model predicted effective diffusivities ranging from 20 to 40% below the experimental diffusivity, depending on the cutoff point for the pore-size distribution. There are insufficient data as yet on the reliability of this model for diffusion in microporous catalysts, however, to comment on whether these values are within the limitations of this model.

Although the differences between the experimental and predicted effective diffusivities can conceivably be regarded as within the limitations of the accuracy of the predictions, there is another possible cause for the observed deviations. The observed differences may be due to a mass transport effect not accounted for in the prediction models and which was not significant in the diffusion measurements made in the absence of reaction. A possible mass transport process which could explain the observation is a surface diffusion phenomenon. Since a chemical reaction on a solid porous catalyst necessitates adsorption of reactants onto the surface and desorption of products from the surface, the transport or movement of some molecules along the surface seems likely. This would be especially true if the desorption activation energy of the products is much larger than the energy required for migration of molecules on the surface. Both surface diffusion and gas-phase diffusion would occur in parallel in the direction of decreasing concentration gradients. If gas-phase diffusion is treated independently of surface diffusion, the latter would be an additive process which would increase the total mass transport rate.

Unfortunately, little is known about the mechanism and extent of surface diffusion in the presence of reaction in a porous catalyst. If surface diffusion is generally significant with a chemical reaction, then the present theoretical diffusion models would be inadequate in predicting the effective diffusivity. Perhaps the best way of determining if effective diffusivities with and without reaction are identical would be to compare diffusivities with reaction with diffusion rates measured in the catalyst under similar conditions but in the absence of reaction, for example, by using an equilibrated gas. This would eliminate the use of prediction models, which are only supported experimentally within large deviations.

VALIDITY OF ASSUMPTIONS

From the literature (*8*), the ortho-para shift of hydrogen on a ferric oxide gel catalyst appears to comply with the assumptions for an easily solvable mathematical model of the effective diffusivity with reaction. The necessary requirements of the model are a first-order isothermal reaction and either equimolar diffusion or conditions of Knudsen flow (*24*). In addition, interparticle diffusion effects must be negligible, and the plug-flow assumption must be valid.

The ortho-para shift of hydrogen is obviously equimolar and produces no side reactions. Hutchinson, et al. (*8*) reported that at liquid nitrogen temperature, both the forward and reverse reactions of the ortho-para shift of hydrogen over a ferric oxide gel catalyst followed Langmuir-Hinshelwood expressions:

$$\overline{R} = \frac{k(C_A - C_{Ae})}{1 + k' C_A} \tag{25}$$

However, from the experimental data of Hutchinson (*8*) and of Barrick, et al. (*1*) the maximum variation of a pseudo-first-order-reaction rate constant

$$K_{rv} = \frac{k}{1 + k' C_A} \tag{26}$$

is less than 10% for the range of parahydrogen concentration encountered in this work (from 0.35 to 0.43 mole fraction). Thus over a small range of parahydrogen concentration the reaction can be considered approximately first-order. A first-order plot for reaction over catalyst 80-02 (see Figure 4) does exhibit first-order kinetics.

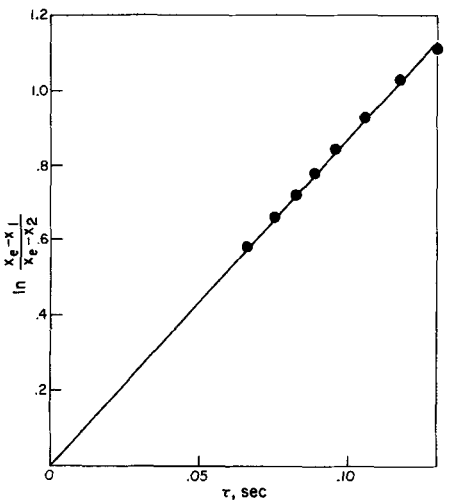

Fig. 4. First-order plot catalyst 80-02.

The works of Hutchinson, et al. (*8*) and Barrick, et al. (*3*) considered at length the questions of isothermality, interparticle diffusion, and dispersion effects for the experimental system used in this study. It was concluded in these works that the reaction was essentially isothermal and diffusion effects were negligible over ranges of experimental conditions for exceeding the range used in the present investigation. One of the authors (*16*) further considered these points with the same conclusions.

CONCLUSIONS

The conclusions from this work are:

1. The experimental effective diffusivities showed a maximum deviation within ± 1.2% from the average over a range of effectiveness factors from 0.78 to 0.96.
2. The theoretical models predicted diffusivities significantly below the effective diffusivities calculated from the sphere model. Although the results from one sample are insufficient to establish quantitatively the relative merits of the models, the results obtained indicate that surface diffusion may be present in addition to gas-phase diffusion.

ACKNOWLEDGMENT

The authors express their appreciation to D. H. Weitzel, who donated the catalyst; to the Shell Companies Foundation and the National Science Foundation for financial support; to R. N. Foster for helpful suggestions in strengthening the paper; and to D. L. Page, for assistance in the solution of mechanical problems.

NOTATION

C = total gas-phase concentration, mole/L^3
C_A = concentration of reactant, mole/L^3
C_{Ae} = equilibrium concentration of reactant, mole/L^3
C_{Ao} = reactant concentration at pore mouth, mole/L^3
d_p = apparent particle density, M/L^3
D_{AB} = molecular diffusivity, L^2/t
D_e = effective diffusivity, L^2/t
D_K = Knudsen diffusivity, L^2/t
D_{pre} = predicted effective diffusivity, L^2/t
E = effectiveness factor
F = feed rate to catalyst chamber, L^3/t
h_{sp} = Thiele Modulus for sphere
k = parameter in Equation (25), L/t
k_s = first-order surface reaction rate constant, L/t
k' = parameter in Equation (25), L^3/mole
K = pore orientation parameter (reciprocal of tortuosity factor)
K_{rv} = pseudo first-order reaction rate constant, L/t
L = length of reaction zone, L
M = molecular weight, M/mole
N_{Az} = molar flux of substance A, mole/L^2t
P_v = pore volume per gram, L^3/M
r = pore radius, L
$\bar{r}$ = mean pore radius, L
r_p = distance from center of catalyst particle, L
R = gas constant, FL/mole T
$\bar{R}$ = rate of consumption of reactant, mole/L^3t
R_p = radius of spherical particle, L
S = surface area per volume of catalyst, L^2/L^3
S_t = surface area of catalyst per gram, L^2/M
S_x = exterior surface area of catalyst particle, L^2
T = absolute temperature, T
$\bar{v}$ = mean molecular velocity, L/t
V_C = catalyst volume, L^3
V_p = apparent volume of catalyst particle, L^3
x_A = mole fraction of reactant
z = distance through catalyst particle, L
α = internal porosity
τ = residence time in reactor, t

LITERATURE CITED

1. American Instrument Co., Inc., *Cat. No. 5-7119*, 8030 Georgia Ave., Silver Spring, Maryland (1965).
2. Aris, R., *Chem. Eng. Sci.*, **6**, 262 (1957).
3. Barrick, P. L., L. F. Brown, and H. L. Hutchinson, University of Colorado, *Air Force Tech. Document. Rept. APL TDR-64-77* Univ. Colorado, Boulder (Sept., 1964).
4. Bird, R. B., W. E. Stewart, and E. N. Lightfoot, "Transport Phenomena," John Wiley, New York, (1962).
5. Glasstone, S., and D. Lewis, "Elements of Physical Chemistry," p. 26, D. Van Nostrand, Princeton, N. J. (1960).
6. Haynes, H. W., Jr., MS thesis, p. 54, Univ. Colorado, Boulder (1966).
7. Henry, J. P., Jr., R. S. Cunningham, and C. J. Geankopolis, *Chem. Eng. Sci.*, **22**, 11 (1967).
8. Hutchinson, H. L., P. L. Barrick, and L. F. Brown, *Chem. Eng. Progr. Symp. Ser. No. 72*, **63**, 18 (1967).
9. Johnson, M. F. L., W. E. Kreger, and H. Erickson, *Ind. Eng. Chem.* **49**, 283 (1957).
10. ———, and W. E. Stewart, *J. Catalysis*, **4**, 248 (1965).
11. Numec Instruments and Controls Corporation, *Model MIC 101*, Apollo, Penn. (1964).
12. Orr, C., Jr., and J. M. Dallavalle, "Fine Particle Measurement," Macmillan, New York (1959).
13. Rao, M. R., and J. M. Smith, *AIChE J.*, **9**, 19 (1963).
14. ———, N. Wakao, and J. M. Smith, *Ind. Eng. Chem. Fundamentals*, **3**, 127 (1964).
15. Satterfield, C. N., and T. K. Sherwood, "The Role of Diffusion in Catalysis," p. 25, Addison-Wesley, Reading, Mass. (1963).
16. Sterrett, J. S., MS thesis, Univ. Colorado, Boulder (1967).
17. Thiele, E. W., *Ind. Eng. Chem.*, **31**, 916 (1939).
18. Wakao, N., and J. M. Smith, *Ind. Eng. Chem. Fundamentals*, **3**, 123 (1964).
19. ———, *Chem. Eng. Sci.*, **17**, 825 (1962).
20. Weisz, P. B., and C. D. Prater, in "Advances in Catalysis," pp. 170-1, Vol. VI, ed., W. G. Frankenburg, V. I. Komarewsky, and E. K. Rideal, Academic Press, New York (1954).
21. ———, and A. B. Schwartz, *J. Catalysis*, **1**, 399 (1962).
22. ———, and E. W. Swegler, *J. Phys. Chem.*, **59**, 823 (1955).
23. Weitzel, D. H., and W. V. Loebenstein, *U. S. Patent 2,943,917*, (July 5, 1960).
24. Wheeler, A., in "Advances in Catalysis," pp. 249-327, Vol. III, ed., W. G. Frankenburg, V. I. Komarwesky, and E. K. Rideal, Academic Press, New York (1951).

Manuscript received August 30, 1967; revision received November 16, 1967; paper accepted November 20, 1967.